Correlation of electrical and optical properties of the vanadium-related *C* level in silicon

R. Pässler*
Fakultät für Naturwissenschaften, Technische Universität Chemnitz-Zwickau, 09107 Chemnitz, Germany

H. Pettersson and H. G. Grimmeiss
Department of Solid State Physics, University of Lund, Box 118, S-221 00 Lund, Sweden

K. Schmalz
Institute of Semiconductor Physics, P.O. Box 409, 15204 Frankfurt (Oder), Germany
(Received 4 August 1995; revised manuscript received 5 August 1996)

Gibb's free energies due to hole transitions between the *C* level of Si:V and the valence band have been determined for eleven different temperatures within the range 190 K$\leqslant T\leqslant$270 K on the basis of simultaneous measurements of corresponding thermal hole capture coefficients and emission rates. Zero-phonon binding energies have been determined from the low-energy part of photoionization cross-section spectra at five different temperatures within the range 75 K$\leqslant T\leqslant$170 K. The temperature dependence of these binding energies can be described by a Varshni-type analytical formula with a zero-temperature level position of $E_v+0.361$ eV ($\pm$0.003 eV). The associated ratio of the temperature-induced change of this level position with respect to the one of the band-gap energy is about 0.80 ($\pm$0.10). The inherent correlation between electrical and optical level position parameters was used to calculate the temperature dependence of the zero-phonon binding energy, $J_p(T)$, the Gibb's free energy, $G_p(T)$, and the enthalpy, $H_p(T)$, from 0 K to room temperature. Using two photoionization cross-section spectra, the associated Franck-Condon shift was estimated to be about 0.04 eV. [S0163-1829(96)00544-9]

I. INTRODUCTION

A reasonable understanding of electrical and optical properties of transition metals in silicon is of considerable interest in view of their wide use in semiconductor electronics. In spite of this interest, it is fair to say that current knowledge about electronic properties of several transition metals is still rather limited. This applies, in particular, to vanadium-related centers in silicon.

During recent years, vanadium-doped silicon has been the subject of a series of experimental as well as theoretical studies (see, in particular, Ohta *et al.*,[1] Tilly *et al.*[2] and references therein). Though differences in published data are observed, particularly with regard to level positions, it is generally agreed[1,2] that vanadium in silicon gives rise to an acceptor level (*A* level) and a donor level (*B* level) in the upper half of the band gap as well as a donor level (*C* level) in the lower half of the band gap.[1] A detailed study of electrical properties in combination with low-temperature measurements of the associated photoionization cross sections[2] provided level positions of about $E_c-0.21$ eV for the *A* level, $E_c-0.48$ eV for the *B* level, and $E_v+0.36$ eV for the *C* level. The consistency of the latter value has recently been confirmed[3] by a detailed theoretical study of the measured photoionization cross-section spectrum of holes, $\sigma_p(h\nu, 77\ \mathrm{K})$, (Fig. 11 in Ref. 2) which resulted in a zero-phonon binding energy of $J_p(77\ \mathrm{K})=0.356$ eV within an uncertainty of about $\pm$0.005 eV.

Optical $\sigma_p(h\nu,T)$ data of the *C* level which would allow the determination of the temperature dependence of the zero-phonon binding energy, $J_p(T)$, are to the best of our knowledge not available from literature. One important goal of this paper has therefore been to present photoionization cross-section spectra for five different temperatures within the range 75 K$\leqslant T\leqslant$170 K and, using these data, to determine the corresponding T dependence of the zero-phonon binding energy, $J_p(T)$. It is shown in Sec. III B that this temperature dependence can be described by a Varshni-type analytical formula.[4,5] By connecting optical level positions with Gibb's free energies derived directly (i.e., without any intermediate exponential regression procedures[2,6]) from ratios of thermal hole emission rates and capture coefficients, we were further able to determine all parameters necessary for a numerical analysis of the temperature dependence of the zero-phonon binding energy, $J_p(T)$, Gibb's free energy, $G_p(T)$, and the associated enthalpy, $H_p(T)$, over an unusually large temperature range ($0\leqslant T\leqslant 300$ K). Furthermore, the extension of our photoionization cross-section measurements to rather low photon energies made it possible to present a reliable estimation of the lattice adjustment energy[7,8] (=Franck-Condon shift[9]) for the vanadium-related *C* level in silicon. This energy is shown to be a factor of about 3 smaller than the one suggested by Ohta and Sakata[10] on the basis of a numerical analysis of their thermal capture and emission data.

Investigations of the kind presented in this paper are considered as an important complement to high-resolution optical spectroscopy studies such as Fourier-transform infrared spectroscopy which, in general, do not provide comprehensive and consistent sets of important thermodynamical entities such as Gibb's free energies, enthalpies, and entropies. In addition, the analytical procedures suggested in this paper offer the possibility to measure zero-phonon binding energies and Franck-Condon shifts for defects with an accuracy

of a few meV without preparing samples exhibiting sharp line spectra together with phonon replicas. We have chosen the C level in Si:V as an example to demonstrate the power of these analysis procedures.

II. EXPERIMENTAL DETAILS

The samples used in this study were vanadium-doped n^+p silicon diodes with a free hole concentration of about 10^{15} cm^{-3}. The diodes were prepared without metallization using a localized oxidation of silicon technology. The n^+ region was prepared by arsenic implantation followed by an annealing at 1100 °C for $2h$. Vanadium (^{51}V) ions with an energy of 300 keV and a dose of 10^{13} cm^{-2} were implanted onto the front side of the wafer. The implanted ions were driven into the p-type region by heating the samples to 1100 °C for 30 min. The vanadium centers were electrically activated by rapid thermal annealing at 1250 °C for 30 s in a nitrogen ambient resulting in a concentration of 10^{14} cm^{-3} vanadium-related centers.

The thermal emission rates were obtained by deep level transient spectroscopy (DLTS) (Ref. 11) at high temperatures and from exponential regressions of single-shot capacitance transients at low temperatures. Since the time constants of corresponding hole capture transients were, depending on the temperature, in the range 50 to 500 μs they could not be registered directly by a regular capacitance meter (Boonton 72B). The standard procedure in this case is to determine indirect hole capture capacitance transients by measuring, depending on the temperature, peak amplitudes in DLTS (Ref. 11) and amplitudes at $t=0$ of emission transients in single-shot capacitance spectroscopy[12] for filling pulses of consecutive increasing length. This combination of various techniques enabled us to measure the emission and capture rates over a fairly large temperature region.

Capture transients are often nonexponential due to the influence of free-carrier tails in the space-charge region. We have fitted our hole capture transients to a theoretical expression taking into account such effects.[13] However, by using a large reverse bias (in our case 8 V) after the filling pulse, the influence of nonexponential effects on capture transients was found to be small.

The optical data were collected by photocapacitance spectroscopy.[12] The experiments were performed using a 0.5-m grating monochromator from Acton Research with an energy resolution of about 1 meV. The setup was fully computerized. To avoid disturbances from strong absorption lines due to, e.g., water, the complete experimental setup including the globar house, monochromator, and optical collimating system was evacuated.

III. EXPERIMENTAL RESULTS AND ANALYTICAL TREATMENTS

A. Emission rates and capture coefficients

Hole emission rates, $e_p(T)$, and associated capture coefficients, $c_p(T)$, were measured at eleven different temperatures between 190 and 270 K (see Table I and Figs. 1 and 2). According to semiconductor statistics,[14–18] hole emission rates, $e_p(T)$, are connected with hole capture coefficients, $c_p(T)$, by a relationship of the form

TABLE I. Measured hole emission rates, $e_p(T)$, and hole capture coefficients, $c_p(T)$, of the C level in Si:V. The fourth and fifth columns show the relevant ratio $e_p(T)/(c_p(T)N_v(T))$ [=argument of the logarithmic function in Eq. (2)] and the resulting Gibb's free-energy values, $G_p(T)$, respectively.

T (K)	e_p (s^{-1})	c_p (cm^3 s^{-1})	$e_p/(c_pN_v)$	G_p (eV)
270.7	605.3	2.043×10^{-11}	3.39×10^{-6}	0.294
262.8	302.7	1.797×10^{-11}	2.01×10^{-6}	0.297
252.5	121.1	1.546×10^{-11}	9.94×10^{-7}	0.301
245.0	60.53	1.294×10^{-11}	6.21×10^{-7}	0.302
235.9	24.21	1.061×10^{-11}	3.21×10^{-7}	0.304
229.6	12.11	9.420×10^{-12}	1.88×10^{-7}	0.306
222.6	6.053	8.463×10^{-12}	1.10×10^{-7}	0.307
215.6	2.421	7.323×10^{-12}	5.32×10^{-8}	0.311
205.5	0.6615	5.782×10^{-12}	1.98×10^{-8}	0.314
198.3	0.2365	4.948×10^{-12}	8.72×10^{-9}	0.317
189.4	0.0645	3.988×10^{-12}	3.16×10^{-9}	0.319

$$\frac{e_p(T)}{c_p(T)}=N_v(T)\exp\left(-\frac{G_p(T)}{k_BT}\right). \tag{1}$$

Here, $G_p(T)$ represents the Gibb's free energy due to hole transitions from a given defect and $N_v(T)=N_v(300\ \mathrm{K})(T/300\ \mathrm{K})^{3/2}$ is the effective density of states in the valence band which in the case of silicon is numerically given by $N_v(300\ \mathrm{K})=1.02\times10^{19}$ cm^{-3}.

Gibb's free energy, $G_p(T)$, in Eq. (1) can be expressed in terms of the measured quantities $e_p(T)$ and $c_p(T)$ as

$$G_p(T)=-k_BT\ \ln\left(\frac{e_p(T)}{c_p(T)N_v(T)}\right). \tag{2}$$

It is evident from Eq. (2) that the quantities $e_p(T)$ and $c_p(T)$ should be measured at the same temperature in order to exclude additional inaccuracies induced by experimental regressions usually performed on such sets of data.[2,6] Measured values of the ratio $e_p(T)/(c_p(T)N_v(T))$ are given in the fourth column of Table I and plotted in Fig. 3. Resulting Gibb's free energies are presented in the last column of Table I (cf. Fig. 6).

B. Photoionization cross sections

Photoionization cross-section spectra, $\sigma_p(h\nu,T)$, due to hole excitation from the C level into the valence band have been measured at five different temperatures. Experimental results for photon energies $h\nu\leqslant0.5$ eV are presented in Fig. 4. The spectra show a pronounced thermal broadening (activation) in the low-energy tail region which is believed to be due to optical-absorption processes assisted by multiphonon (MP) emission and absorption. A detailed theoretical analysis and interpretation of such spectra is rather complicated in the case of hole excitation from deep levels in silicon due to the valence-band degeneracy and particularly in view of the onset of the split-off band at a distance of only 40 meV from the valence-band edge. On the other hand, it has been demonstrated previously[3,18–21] that it is nevertheless possible to deduce basic information from thermally broadened photoionization cross-section spectra (like those presented in Fig.

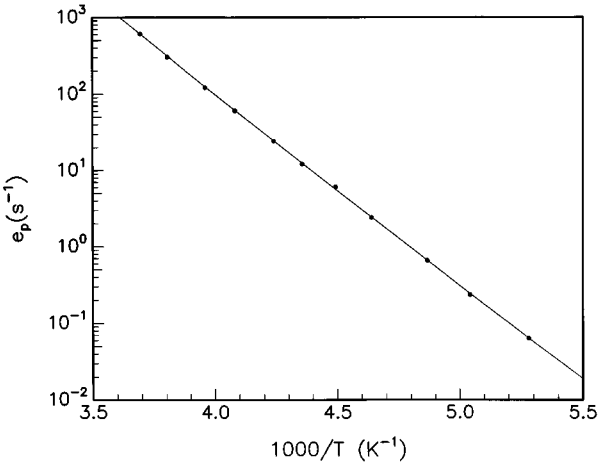

FIG. 1. Graphical representation of the temperature dependence of the experimental hole emission rates, $e_p(T)$ (second column of Table I) for the C level in Si:V. The continuous curve represents the results of a detailed numerical fitting of the experimental $e_p(T)$ and $c_p(T)$ data (Table I) on the basis of the theory of NMP transitions (Ref. 35) with appropriately chosen parameters for the lattice adjustment energy A and the phonon energy $h\omega$ (in analogy to Ref. 10). An approximate fitting of this curve by a dependence (Ref. 2) of type $e_p(T)\propto T^2\exp(-E_p^{\uparrow}/k_BT)$ (17) gives a conventional (effective) activation energy of $E_p^{\uparrow}\cong 458$ meV for this hole emission process.

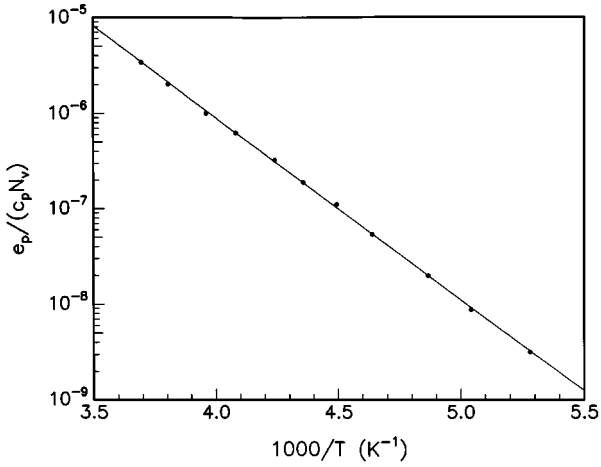

FIG. 3. Graphical representation of the temperature dependence of the ratio $e_p(T)/(c_p(T)N_v(T))$ (fourth column of Table I) for the C level in Si:V. The continuous curve represents the results of a numerical fitting of this ratio on the basis of Eqs. (5) and (10) with appropriately chosen parameters α_p, g_n/g_p, and $J_p(0)$ (cf. subsection III A). An approximate fitting of this curve by $e_p(T)/(c_p(T)N_v(T))\propto\exp(-H_p/k_BT)$ (of Arrhenius type) gives an average activation energy of $H_p\cong 378$ meV corresponding to the difference $E_p^{\uparrow}-E_p^{\downarrow}$ (see captions of Figs. 1 and 2). This effective enthalpy value (visualized by a cross in Fig. 6) is equal to the calculated enthalpy value of $H_p(240\text{ K})=378$ meV using Eq. (16).

4) without using the total analytical theory of MP-activated photoionization cross sections (see, e.g., Refs. 22–29 and Sec. IV). This is particularly true for estimations of zero-phonon binding energies, $J_p(T)$.[3,18,19]

The essence of this procedure of estimating zero-phonon binding energies is based on the observation that thermally broadened $\sigma(h\nu,T)$ curves are described by a photon energy dependence $\exp(h\nu/2k_BT)$ in the vicinity of the zero-phonon binding energy. Equivalently, we can state that a transformed curve of the form[3,18–21]

$$\rho(h\nu,T)\equiv\exp\left(-\frac{h\nu}{2k_BT}\right)\sigma(h\nu,T) \tag{3}$$

tends to have a maximum at a position $h\nu^{(\rho)}(T)$ which should only be a few k_BT higher[3,18] than the corresponding zero-phonon binding energy, $J(T)$. A detailed study of the actual peak position of $\rho_p(h\nu,T)$ curves in the case of repulsive centers[3] has shown that the energy distance of $h\nu_p^{(\rho)}(T)$ with respect to $J_p(T)$ is approximately[3] given by

$$\Delta_p^{(\rho)}(T)\equiv h\nu_p^{(\rho)}(T)-J_p(T)\cong\left(\sqrt[3]{(\pi^2R_p^{+1}/2k_BT)}+\frac{5}{12}\right)2k_BT. \tag{4}$$

This relation is valid within the usual regime of a nonvanishing component of allowed transitions which dominates at least in the immediate vicinity of the electronic absorption edge. Here, R_p^{+1} ($\approx$15 meV for a donor level in a +1 charge state in silicon) represents the Rydberg energy characterizing the strength of a repulsive barrier which has to be tunneled by a hole during excitation into the light-hole band. A closer inspection of the transformed $\rho_p(h\nu,T)$ curves in Fig. 5 results in approximate vertex positions (within uncertainties of a few meV) at the $h\nu_p^{(\rho)}(T)$ values listed in the second column of Table II. By subtracting the theoretical shift values, $\Delta_p^{(\rho)}(T)$, [Eq. (4), listed in the third column of Table II] from the $h\nu_p^{(\rho)}(T)$ values one obtains the approximate zero-phonon binding energies, $J_p(T)$, listed in the fourth column

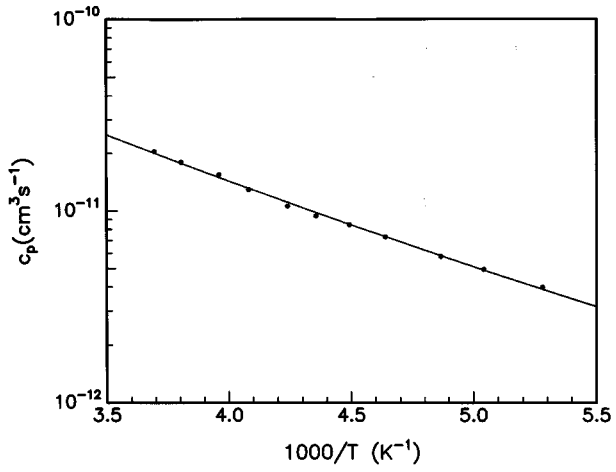

FIG. 2. Graphical representation of the temperature dependence of the experimental hole capture coefficients, $c_p(T)$ (third column of Table I) for the C level in Si:V. The continuous curve represents (in analogy to Fig. 1) the results of a detailed numerical fitting of $e_p(T)$ and $c_p(T)$ data on the basis of the theory of NMP transitions (Ref 35). An approximate fitting of this curve by a dependence (Ref. 2) of type $c_p(T)\propto T^{1/2}\exp(-E_p^{\downarrow}/k_BT)$ (18) gives a conventional (effective) activation energy of $E_p^{\downarrow}\cong 80$ meV for this hole capture process.

TABLE II. Vertex position values, $h\nu_p^{(\rho)}(T)$, rest distance values, $\Delta_p^{(\rho)}(T)$, and the resulting zero-phonon binding energies, $J_p(T)$ (the remaining uncertainties of the latter are confined to about ± 0.003 eV).

T (K)	$h\nu_p^{(\rho)}$ (eV)	$\Delta_p^{(\rho)}$ (eV)	J_p (eV)
170.5	0.410	0.063	0.347
137.6	0.406	0.054	0.352
119.0	0.403	0.048	0.355
95.0	0.397	0.041	0.356
75.0	0.392	0.035	0.357

of Table II. These values are indicated by vertical bars in Fig. 5 and filled circles in Fig. 6.

C. Correlation of thermal and optical results

Theoretical analyses of MP-assisted photoionization cross-section spectra as well as of nonradiative multiphonon (NMP) capture and emission rates are usually based on the assumption[3,7,18,21,23,24,29–35] that the phonon energies of the relevant vibrational modes remain unchanged during the change of the charge state (carrier excitation). Given this assumption, Eq. (1) can be rewritten as[7,31,35]

$$\frac{e_p(T)}{c_p(T)} = \frac{g_n}{g_p} N_\nu(T) \exp\left(- \frac{J_p(T)}{k_B T} \right) \tag{5}$$

where g_n and g_p are the statistical weights (degeneracy factors) of the trap level in the charge state ''full'' (trapped electron) and ''empty'' (trapped hole), respectively. Hence, by comparing Eqs. (2) and (5) it is evident that the Gibb's free energy, $G_p(T)$, is connected with the associated zero-phonon binding energy, $J_p(T)$, by the relation

$$G_p(T) = J_p(T) - S_p^e T, \tag{6}$$

where[16–18]

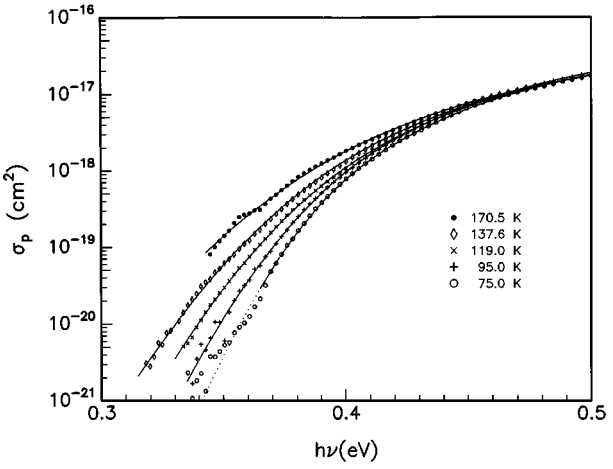

FIG. 4. Experimental photoionization cross-section spectra, $\sigma_p(h\nu)$, due to hole excitation from the C level in Si:V at five different temperatures.

$$S_p^e \equiv k_B \ln\left(\frac{g_n}{g_p} \right) \tag{7}$$

represents the electronic entropy part. Hence, the difference between $G_p(T)$ and $J_p(T)$ should be proportional to T. At the same time, it is obvious from Fig. 6 that the T dependence of $J_p(T)$ is nonlinear (nearly quadratic), at least within the studied temperature interval between 75 and 170 K. Such a nonlinear behavior is not surprising in view of the fact that by definition[19,35,36] the sum of the complementary zero-phonon binding energies, $J_n(T)$ and $J_p(T)$, must be equal to the width of the energy-band gap, $E_{cv}(T)$,

$$J_n(T) + J_p(T) \equiv E_{cv}(T). \tag{8}$$

The T dependence of $E_{cv}(T)$ can be approximated by Varshni's formula[4,5]

$$E_{cv}(T) = E_{cv}(0) - \alpha_{cv} \frac{T^2}{T+\beta}, \tag{9}$$

where $\alpha_{cv} = 4.730 \times 10^{-4}$ eV K^{-1}, $\beta = 636$ K, and $E_{cv}(0) = 1.170$ eV for Si.[5] At least one of the two complementary functions $J_n(T)$ or $J_p(T)$ should exhibit a pronounced nonlinear (quadratic) T dependence at $T \ll \beta$. For an approximate analytical description of this T dependence, a Varshni-type ansatz is again used (in analogy with Refs. 3, 18, 19),

$$J_p(T) = J_p(0) - \alpha_p \frac{T^2}{T+\beta}. \tag{10}$$

Here, the relative shrinkage ratio α_p/α_{cv} can be expected to be in the range between 0 and 1. Within this analytical approximation [Eq. (10)], the associated Gibb's free energy [Eq. (6)] is explicitly given by an expression of the form

$$G_p(T) = J_p(0) - \alpha_p \frac{T^2}{T+\beta} - S_p^e T. \tag{11}$$

Inspecting the analytical expressions of zero-phonon binding energies, $J_p(T)$, and Gibb's free energies, $G_p(T)$, it is realized that one is concerned with a total set of only three (center-specific) parameters, which may easily be determined by simultaneously fitting the sets of calculated $G_p(T)$ values (listed in Table I) and estimated $J_p(T)$ values (listed in Table II). The resulting parameters are (i) an absolute shrinkage coefficient value of $\alpha_p = 3.67 \times 10^{-4}$ eV K^{-1} corresponding to a relative shrinkage ratio α_p/α_{cv} of about 0.78 (± 0.10) between the energy-level position and the energy-band gap, (ii) an electronic entropy part of $S_p^e = 1.37 \times 10^{-4}$ eV K^{-1} ($= 1.6 k_B$) corresponding to a degeneracy ratio of $g_n/g_p = 4.9$, and (iii) a zero-temperature level position $J_p(0) = 0.361$ eV (± 0.003 eV).

The numerical fitting of the three basic parameters α_p, S_p^e, and $J_p(0)$ enables one to determine the T dependence of the associated enthalpy, $H_p(T)$, and the total entropy, $S_p(T)$. The latter is generally defined as

$$S_p(T) \equiv - \frac{\partial G_p(T)}{\partial T} = S_p^a(T) + S_p^e, \tag{12}$$

where[18]

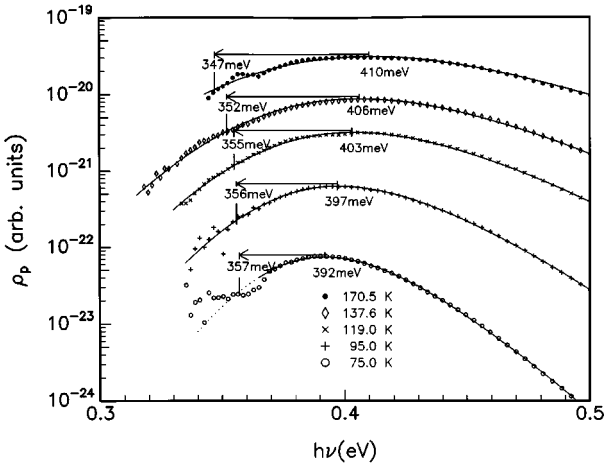

FIG. 5. Transformed $\rho_p(h\nu,T)$ curves due to a transformation according to Eq. (3). The reference point $h\nu_r$ (Refs. 3, 18) controlling their mutual distances in vertical direction has been chosen to be 0.28 eV. The arrows indicate the characteristic energy distances, $\Delta_p^{(\rho)}(T)$ [Eq. (4)] (third column in Table II) between vertex positions, $h\nu_p^{(\rho)}(T)$, and the corresponding zero-phonon binding energies, $J_p(T)$ (fourth column in Table II).

$$S_p^a \equiv -\frac{\partial J_p(T)}{\partial T} = \alpha_p \frac{T(T+2\beta)}{(T+\beta)^2} \tag{13}$$

according to Eqs. (6) and (10) and in analogy to Ref. 5 represents the ''atomic'' part[17,18] of the entropy change due to the shrinkage of $J_p(T)$. The T dependence of the corresponding total entropy, $S_p(T)$ [Eq. (12)] together with its two qualitatively different components $S_p^a(T)$ [Eq. (13)] and S_p^e [Eq. (7)] are shown in Fig. 7.

The associated enthalpy is generally defined as[16,17]

$$H_p(T) \equiv G_p(T) + S_p(T)T, \tag{14}$$

which can, according to Eqs. (6) and (12), also be written in the form[3]

$$H_p(T) = J_p(T) + S_p^a(T)T. \tag{15}$$

The latter reduces according to Eqs. (10) and (13) to the analytical form

$$H_p(T) = J_p(0) + \alpha_p\beta\left(\frac{T}{T+\beta}\right)^2, \tag{16}$$

again in analogy with Ref. 5. The corresponding $H_p(T)$ curve is presented in Fig. 6. It is readily seen that $H_p(T)$ near the middle part of the temperature region, in which the experiments were performed, amounts to $H_p(240\ \mathrm{K}) = 0.378$ eV (indicated by a cross in Fig. 6). This value corresponds to the effective (conventional) activation energy of the $e_p/(c_pN_v)$ curve in Fig. 3.

IV. DISCUSSION

One of the goals of this study was to collect very carefully thermal emission rates and capture coefficients for the C level of vanadium-related centers in silicon in the temperature range 190 K$\leqslant T \leqslant$270 K (cf. Table I). The temperatures have been chosen to be exactly the same for both series of measurements. This unconventional procedure enabled us to determine values of Gibb's free energy, $G_p(T)$, which are not affected by any numerical or graphical manipulation. The values obtained in this way are somewhat different from those presented in Ref. 2 (indicated in Fig. 6 by a dotted line). Comparing the previous data with present results (represented by open circles in Fig. 6), it is realized that the present $G_p(T)$ values within the temperature range 190 K$\leqslant T \leqslant$270 K are about 10–20 meV smaller than the ones given in Ref. 2 and that the $G_p(T)$ values presented in this paper decrease more strongly with increasing temperature than the previous ones. Furthermore, a total entropy of $S_p(240\ \mathrm{K}) \cong 3.6k_B$ (cf. Fig. 7) has been obtained near 240 K, which is about a factor of 2 higher than the value of $1.7k_B$ reported in Ref. 2. The associated enthalpy value $H_p(240\ \mathrm{K})$ [represented in analogy to Ref. 5 by the intersection point of the 240 K tangents to the $G_p(T)$ and $J_p(T)$ curves with the energy axis in Fig. 6] is about 378 meV. This value is 19 meV higher than the approximate enthalpy value of 359 meV obtained in Sec. III of Ref. 2 by using conventional fitting procedures.

The origin of this difference between present and earlier enthalpy values is almost exclusively due to different experimental $e_p(T)$ and $c_p(T)$ data and not due to the unconventional and more elaborate character of the present analysis procedure (Sec. III). Fitting our thermal emission rates, $e_p(T)$ (cf. Table I) to an Arrhenius-type expression,

$$\frac{e_p(T)}{T^2} \propto \exp\left(-\frac{E_p^{\uparrow}}{k_BT}\right), \tag{17}$$

one obtains by using the same exponential regression procedure as in Ref. 2 a conventional activation energy of $E_p^{\uparrow} \cong 458$ meV for the hole emission. This value is 11 meV higher than the 447 meV calculated from Fig. 9 in Ref. 2. Since the present and previous measurements were performed with different reverse bias, this difference may be explained by a small Poole-Frenkel shift.[37] Furthermore, a fitting of the normally employed hole capture cross section $\sigma_p(T) = c_p(T)/v_p(T)$ (Ref. 2) [where $v_p(T) \propto T^{1/2}$ is some average thermal hole velocity] to a conventional Arrhenius-type expression

$$\sigma(T) \propto \frac{c_p(T)}{\sqrt{T}} \propto \exp\left(-\frac{E_p^{\downarrow}}{k_BT}\right), \tag{18}$$

results in a conventional activation energy of $E_p^{\downarrow} \cong 80$ meV for the hole capture. This value is 8 meV lower than the 88 meV calculated from Fig. 10 in Ref. 2. This discrepancy may partly be explained by the increased accuracy in the present measurements as well as the refined analysis procedure. It should, however, be kept in mind that the accuracy in this kind of measurements is generally considered to be 10–20 meV. The difference $E_p^{\uparrow} - E_p^{\downarrow}$ gives an effective enthalpy value of $H_p = 378$ meV which, according to Fig. 6, coincides with the enthalpy value, $H_p(T)$, calculated for $T = 240$ K on the basis of our more elaborate numerical analysis in Sec. III.

One of the most important features of the present work compared with previous studies is the measurement of photoionization cross sections, $\sigma_p(h\nu,T)$, which includes a

relatively large number of measurement points in the tail regions at different temperatures. The detailed $\sigma_p(h\nu)$ measurements have been performed at five different temperatures (between 75 and 170 K) which enabled us to calculate[3] a corresponding series of zero-phonon binding energies, $J_p(T)$ (listed in Table II). These values confirmed on the one hand a previous estimation[3] of about 356 meV for $J_p(77\ \mathrm{K})$. Moreover, the actual T dependence of the zero-phonon binding energy, $J_p(T)$, is now fairly well established within the temperature range 75–170 K. A plot of these values (Fig. 6) clearly indicates a quadratic temperature dependence. This is in agreement with what one would expect (cf. Ref. 18 and subsection III C) since T dependencies of zero-phonon binding energies should be described approximately by analytical expressions of Varshni's type.[4,5] By analyzing the temperature dependence of $J_p(T)$, a relative shrinkage ratio, α_p/α_{cv} of about 0.8 is obtained, i.e., a large part of the total shrinkage of the energy-band gap, $E_{cv}(T)[=J_n(T)+J_p(T)]$, is absorbed by $J_p(T)$. This is a significant result in view of the relatively small value of $J_p(T)$ which is only about $E_{cv}/3$. In this context, it should be mentioned that shallow donors use to be pinned to the conduction-band edge. Hence, the observed trend seems even to be valid for deeper donor levels.

A further qualitatively new result of the present paper is the explicit analytical connection (in subsection III C) of thermal measurements [$G_p(T)$ values from Table I] and optical measurements [$J_p(T)$ values from Table II]. This procedure made it possible to perform reliable extensions of experimental data into T regions not covered by corresponding experiments, i.e., to extend the $J_p(T)$ curve from low to intermediate temperatures and, conversely, to extend the $G_p(T)$ curve from intermediate to low temperatures. The latter illustrates the expected linear T dependence[18] of $G_p(T)-G_p(0)\rightarrow -S_p^e\cdot T$ in the $T\rightarrow 0$ limit. This technique allowed us to determine the temperature dependence of the zero-phonon binding energy, $J_p(T)$, the Gibb's free energy, $G_p(T)$, and the enthalpy $H_p(T)$ (cf. Fig. 6) as well as the associated entropy $S_p(T)$ (Fig. 7) for a deep center over a relatively large temperature interval (i.e., between 0 K and room temperature).

The improved accuracy of present versus previous[2] data enabled us to perform a simultaneous fitting of present $G_p(T)$ data (Table I and empty circles in Fig. 6) and $J_p(T)$ data (Table II and filled circles in Fig. 6), which made it possible to determine a unique set of parameters α_p, S_p^e, and $J_p(0)$ on the basis of Eqs. (10) and (11), respectively. The very good agreement between both of these series of experimental level position data and the resulting fit (cf. full curves in Fig. 6) may be taken as a strong indication for a high degree of adequacy and internal consistency of these data.

The determination of zero-phonon binding energies, $J_p(T)$, from T-dependent slopes of photoionization cross-section spectra was, similarly to the one in Ref. 3, based on the assumption that the vanadium-related C level should be repulsive and singly charged for hole transitions between the C level and the valence band, i.e., it should have the character of a second donor level.[36] Since the possible alternative of a neutral center (corresponding to the model of a first donor level[36]) has not definitively been excluded by earlier experimental studies, it might therefore be of interest to check whether or not this alternative can be ruled out on the basis of the present results.

It is realized that the determination of $G_p(T)$ from thermal measurements (Table I) is by definition completely independent of the actual charge state. The associated $J_p(T)$ values determined from measured vertex positions $h\nu_p^{(\rho)}(T)$ of given $\rho_p(h\nu,T)$ curves (Fig. 3) are, however, dependent on the assumption of the underlying charge state. For neutral centers, it has been shown[18] that the characteristic energy difference, $\Delta_p^{(\rho)}(T)$, between $h\nu_p^{(\rho)}(T)$ and $J_p(T)$ in the case of a nonvanishing allowed component reduces to about $2k_BT$. Using these $\Delta_p^{(\rho)}(T)$ values for neutral centers, apparent $J_p(T)$ values ranging between 0.379 eV and 0.381 eV would have been obtained. By combining these tentative $J_p(T)$ values with given $G_p(T)$ values (Table I) and performing again a simultaneous numerical fitting [on the basis of Eqs. (10) and (11), respectively], the C level is found to be almost pinned to the valence band ($\alpha_p\rightarrow 0$) at an energy position of about $E_v+0.38$ eV. This implies that the atomic vibrational part $S_p^a(T)$ almost vanishes [Eq. (13)] and the entropy value of $S_p(240\ \mathrm{K})\cong 3.6k_B$ is exclusively due to the electronic part S_p^e (i.e., $S_p^e\rightarrow 3.6k_B$). This corresponds, according to Eq. (7), to a degeneracy factor ratio of $g_n/g_p\approx 36$. In view of this obviously unreasonably large ratio, and also from more detailed analyses (see below), the tentative model of a first donor level can most probably be excluded.

The lattice adjustment energy A [=Franck-Condon shift $\equiv d_{F.\text{-}C.}$ (Ref. 9)] can approximately be determined by using a graphical method which has been suggested in Ref. 8. This method is analogous to the one for estimations of zero-phonon binding energies (cf. subsection III B).[3,18,19] It is based on the observation[8] that a characteristic $h\nu$ value, $J(T)-A$, exists at which thermally broadened $\sigma(h\nu,T)$ curves can be described by the photon energy dependence $\exp(h\nu/k_BT)$. Again, this is equivalent to the statement that a transformed curve of type[8]

$$\pi_p(h\nu,T)\equiv\exp\left(-\frac{h\nu}{k_BT}\right)\sigma_p(h\nu,T) \tag{19}$$

tends to have a peak at a position $h\nu_p^{(\pi)}(T)$, which is relatively close to the characteristic point $J_p(T)-A$.[8] An analytical estimation of the energy difference $\Delta_p^{(\pi)}(T)$ in the case of repulsion can readily be performed analogous to the one for $\Delta_p^{(\rho)}(T)$ in Ref. 3. For a nonvanishing component of allowed transitions, this leads to the analytical expression

$$\Delta_p^{(\pi)}\equiv h\nu_p^{(\pi)}-[J_p(T)-A]\cong\left(\sqrt[3]{(\pi^2R_p^{+1}/k_BT)}+\frac{5}{12}\right)k_BT. \tag{20}$$

It should be noted that the only difference between the analytical expressions of Eqs. (4) and (20) is the substitution of $2k_BT$ by k_BT. Figure 8 presents the $\pi_p(h\nu,T)$ transformations of the $\sigma_p(h\nu,T)$ curves of Fig. 4. Unfortunately, three of these curves do not extend to sufficiently low photon energies and are not accurate enough to clearly exhibit the expected peak behavior. However, at least the $\pi_p(h\nu)$ curves for $T=137.6$ and 119.0 K exhibit vertex positions at about 0.347 and 0.348 eV, respectively, with an accuracy of about ± 0.01 eV. Furthermore, from Eq. (20) follows that the

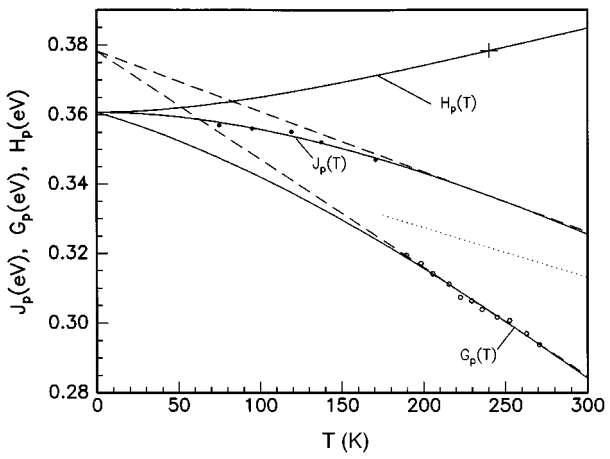

FIG. 6. Analytical approximations of the T dependence of the zero-phonon binding energy, $J_p(T)$ [Eq. (10)] Gibb's free energy, $G_p(T)$ [Eq. (11)], and the associated enthalpy, $H_p(T)$ [Eq. (16)]. The temperature dependencies have been obtained by simultaneous numerical fittings of given $J_p(T)$ values (fourth column of Table II) and $G_p(T)$ values (fifth column of Table I) on the basis of Eqs. (10) and (11).

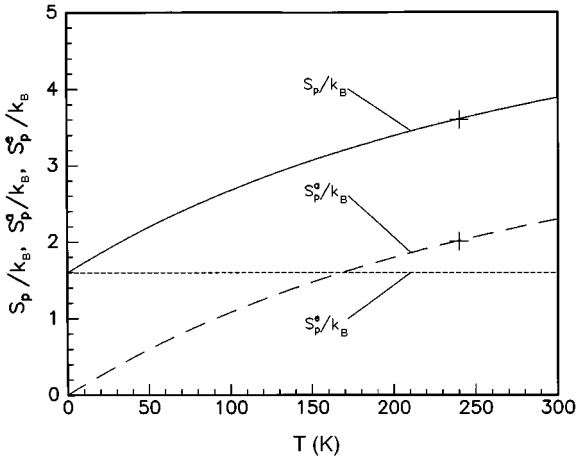

FIG. 7. Temperature dependence of the total entropy change, $S_p(T)$ [Eq. (12)] corresponding to the sum of an ''atomic'' component, $S_p^a(T)$ [Eq. (13)], and a temperature-independent electronic component, S_p^e [Eq. (7)], in units of the Boltzmann constant k_B.

energy shifts are 0.032 and 0.029 eV, respectively. In this way, characteristic positions of $J_p(137.6)-A\cong 0.315$ eV, and $J_p(119.0\ \mathrm{K})-A\cong 0.319$ eV are found. Comparing these values with the corresponding $J_p(T)$ positions (listed in Table II), we obtain adjustment energies, A, of only about 0.036 or 0.037 eV (with a maximum uncertainty of ± 0.010 eV).

This rough graphical estimation can be confirmed by detailed numerical fittings on the basis of a convolution which is given by[3,18,21]

$$\sigma_p(h\nu,T)=\int d(h\tilde{\nu})\tilde{\sigma}_p(h\tilde{\nu})R(h\nu-h\tilde{\nu},T). \qquad (21)$$

Here, the factor $\tilde{\sigma}_p(h\tilde{\nu})$ is the electronic cross section due to the absorption of photons of energy $h\tilde{\nu}\geqslant J_p(T)$ by the electronic subsystem (in this case holes excited into the valence band). The second factor in the convolution integral is the thermally averaged Franck-Condon factor,[7,18] which quantifies the probability that the remaining energy difference $h\nu-h\tilde{\nu}$ is compensated by the emission $(h\nu-h\tilde{\nu}\geqslant 0)$ or absorption $(h\nu-h\tilde{\nu}\leqslant 0)$ of phonons of the vibrational subsystem due to corresponding MP transitions.[7] In view of the fact that the valence band in silicon consists of a light-hole, a heavy-hole, and a split-off band the electronic part $\tilde{\sigma}_p(h\tilde{\nu})$ in Eq. (21) can, in general, be considered to be given by a linear combination [in analogy to Si:S (Ref. 41) and Si:Se (Ref. 42)] of contributions $\tilde{\sigma}_{p_i}(h\tilde{\nu})$, $i=1$, 2, and 3, representing hole excitations into the corresponding subbands. Due to the repulsive $(+1)$ charge of the center after hole excitation, the analytical form of these three components $\tilde{\sigma}_{p_i}^{+1}(h\tilde{\nu})$ is governed by band-specific Sommerfeld factors $s_{p_i}^{+1}(h\tilde{\nu}-J_p)$, $i=1$, 2, and $s_{p_3}^{+1}(h\tilde{\nu}-J_p-\Delta_{so})$ (Refs. 3, 41–43) in the vicinity of the corresponding electronic absorption edges J_p and $J_p+\Delta_{so}$, respectively. $\Delta_{so}=0.04$ eV represents the corresponding spin-orbit splitting in silicon. Using combinations of these Sommerfeld factors with associated neutral parts (represented in analogy to Refs. 41 and 42 by a Taylor series with adjustable expansion coefficients), we have performed a series of alternative fittings of the experimental data (Fig. 4) on the basis of Eq. (21). The lattice adjustment energy, A, was found to amount to about 0.042 ± 0.005 eV. This is in fair agreement with the value estimated above on the basis of the simple graphical procedure[8] (cf. Figs. 5 and 8). The associated effective phonon energy was calculated to be $\hbar\omega=0.017$ eV (± 0.001 eV), which is consistent with results obtained by Ohta and Sakata from numerical analyses of electrical data.[10] Moreover, our detailed numerical analyses resulted in zero-phonon binding energies, $J_p(T)$, which were about 0.001 to 0.002 eV smaller than the ones obtained on the basis of the simpler graphical method[3] (see Table II).

Combining a Franck-Condon shift of about 0.042 eV with an effective hole binding energy $J_p(240\ \mathrm{K})$ of about 0.336 eV (Fig. 6), we are now able to construct a configuration coordinate diagram for the C level of Si:V [Fig. 9(a)]. This diagram shows, in particular, that the classical (high-temperature) capture barrier, given by $(J_p-A)^2/4A$ (Refs. 7, 32, 36, 39) and which determines the efficiency of the non-radiative multiphonon (NMP) carrier capture mechanism,[30–36,39] is of the order of 0.52 eV in the present case of hole capture into the C level of Si:V. This classical barrier height estimated on the basis of optical data is, however, 6–7 times larger than the effective NMP hole capture activation energy (of about $E_p^{\downarrow}\cong 0.08$ eV) derived from the corresponding hole capture cross sections in Fig. 2. Such simple considerations already show that there are obviously great difficulties in presenting a consistent quantum-mechanical interpretation of the optical and electrical properties of the C level.

In accordance with these simple considerations, a detailed theoretical analysis on the basis of a representative theory for NMP carrier capture and emission processes at deep traps in semiconductors (see e.g., Refs. 30–36) shows that a lattice adjustment energy of only 0.04–0.05 eV is much too small to explain the experimentally observed values of $c_p(T)$ (Fig. 2). Hence, in the case of the C level of Si:V we are actually

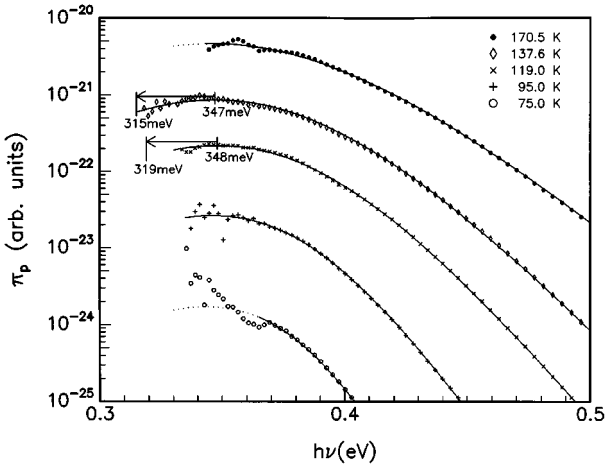

FIG. 8. Transformed $\pi_p(h\nu,T)$ curves due to a transformation according to Eq. (19). The reference point, $h\nu_r$, controlling their mutual distances in a vertical direction, has been chosen to be 0.30 eV. The arrows indicate the characteristic energy distances, $\Delta_p^{(\pi)}(T)$ [Eq. (20)], between vertex positions, $h\nu_p^{(\pi)}(T)$, and the corresponding characteristic positions, $J_p(T)-A$.

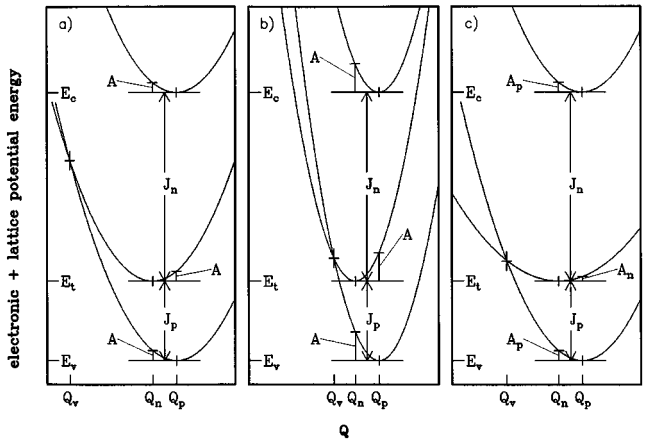

FIG. 9. Different configuration coordinate diagrams of the *C* level in Si:V obtained from different numerical analysis procedures. (a) Diagram based on a Franck-Condon shift of $A=0.042$ eV, which has been determined from a detailed numerical analysis of our optical data (Fig. 4) using Eq. (21). (b) Diagram based on a Franck-Condon shift value of $A\approx0.12$ eV (see Ref. 10 and Sec. IV), which is required in numerical fittings of the experimentally observed activation behavior of electrical data, i.e., hole emission rates (Fig. 1 of this paper or Fig. 6 in Ref. 10) and hole capture coefficients (Fig. 2 of this paper in combination with Fig. 10 of Ref. 10) on the basis of the conventional theory of NMP transitions (Ref. 35) (i.e., for unchanged phonon energy spectra). (c) Diagram obtained from a numerical fit of the same set of electrical data as in (b), but within a more general analytical framework (Refs. 40, 44, 45) of the theory of NMP transitions (envisaging a significant oscillator frequency shift). For a fixed ''empty'' state adjustment energy of $A_p=0.042$ eV in accordance with (a) and Fig. 8, an associated ''full'' state adjustment energy $A_n=0.019$ eV is required in order to produce an equally good alternative fit of the electrical data in consideration.

concerned with a basic discrepancy between different theoretical interpretations of experimentally observed electrical and optical properties of a deep trap that is qualitatively of the same type as the one encountered in the more familiar case of the GaP:O center.[39,40,44]

A qualitatively different configuration coordinate diagram of the Si:V center in question has been proposed by Ohta and Sakata [see Fig. 9(b) which corresponds basically to Fig. 11 of Ref. 10]. Applying a detailed numerical analysis to their $e_p(T)$ and $c_p(T)$ data[10] (which are roughly comparable with the ones listed in Table I) on the basis of NMP transitions for vanishing phonon energy shifts,[35] these authors obtained a lattice adjustment energy, *A*, of about 0.12 eV and an effective phonon energy[7] of 0.017 eV. In order to check the consistency of their parameters[10] with our electrical data (Table I), we combined our $c_p(T)$ curve (Fig. 2) with its somewhat more extended counterpart of Ohta and Sakata (Fig. 10 of Ref. 10) and performed a different fit of these data on the basis of a similar analytical framework.[35] This fitting resulted in nearly the same parameter set for NMP transitions as in Ref. 10, namely, a lattice adjustment energy of 0.12–0.13 eV [see Fig. 9(b)] and an effective phonon energy of 0.016–0.018 eV. The corresponding classical barrier height for NMP capture has actually been confirmed to be in the range 0.09 to 0.10 eV which is close to the effective activation energy obtained from Fig. 2. Thus, in the case of the *C* level of Si:V we are indeed concerned with an unusually pronounced discrepancy between the relatively large value of 0.12–0.13 eV for the lattice adjustment energy derived from numerical fittings of electrical data and the considerably smaller value of 0.04–0.05 eV directly obtained from the shapes of the low-energy tails of the corresponding photoionization cross-section curves.

Concerning this discrepancy between lattice adjustment energy values extracted from electrical and optical data, respectively, it is interesting to assess an earlier estimation of this crucial parameter by Ohta *et al.*[1] on the basis of their hole photoionization cross-section data. The value which they obtained seemed to be in accordance with the relatively, large value of $A\approx0.12$–0.13 eV estimated from their electrical data [cf. Fig. 9(b) with Fig. 9 in Ref. 1]. A closer look on these earlier optical data (Fig. 7 in Ref. 1) shows, however, that they are all confined to a range of relatively high photon energies, i.e., $h\nu>0.43$ eV, where MP broadening effects are much weaker than in the range 0.32–0.40 eV studied in this paper (cf. Figs. 4, 5, and 8). Moreover, our detailed numerical analyses of the optical data presented in Fig. 4 showed that the electronic part $\tilde{\sigma}_p(h\tilde{\nu})$ of the hole excitation cross section, $\sigma_p(h\nu,T)$, has a rather complicated energy dependence which cannot be represented by a single-band model like the one proposed in Ref. 1, which was simply given by the product of a unique Sommerfeld factor (Coulomb factor) and a neutral part of conventional form[29] [corresponding exclusively to forbidden transitions; see Eqs. (6)–(9) in Ref. 1].

In order to study the electronic part in more detail, we have considered larger regions of experimental hole cross-section data. For the lowest-temperature $T=75$ K measurement points up to about 0.64 eV were included [see Fig. 10(a)]. The corresponding fitting (deconvolution) procedure of this enlarged set of experimental data on the basis of Eq. (21) gives the energy dependence of the electronic part over a fairly large interval. The spectral distribution of $\tilde{\sigma}_p(h\tilde{\nu})$ is shown logarithmically by the dashed curve in Fig. 10(a), and

in linear representation by the dashed curve in Fig. 10(b). Examining the shape of the latter curve carefully, one distinguishes three characteristic sections for which the curvature is qualitatively different. For energies $h\nu<0.42$ eV, for which the curve is governed by repulsive barriers, the curvature is relatively strong. A similar curvature is observed at higher energies, 0.50 eV $<h\nu<0.65$ eV, at which the curve is approximately of exponential form. This is markedly different from the relatively weak curvature (almost linear dependence) in the intermediate energy region, 0.44 eV $<h\nu<0.48$ eV. The nearly discontinuous change of curvature becomes more obvious from the first derivative of the spectral distribution, $d\tilde{\sigma}_p(h\nu)/d(h\nu)$, as shown by the dashed curve in Fig. 10(c). A further interesting detail of this curve is a certain steplike structure in the immediate vicinity of 0.40 eV, which seems to be due to the threshold of a second excitation process.

Interestingly, the point of this first derivative curve at which the curvature changes from convex to concave behavior coincides almost with the expected position of the electronic absorption threshold, $J_p(77\text{ K})+\Delta_{so}=0.396$ eV, due to hole excitations into the split-off band. Comparing this result with possible alternative models like those in Refs. 41 and 42, we found that an adequate interpretation of the rather complicated energy dependence of the electronic absorption cross section $\tilde{\sigma}_p(h\nu)$ can be given up to about 0.45 eV on the basis of allowed transitions into the light-hole band[3] [starting at $J_p(77\text{ K})=0.356$ eV] in conjunction with allowed transitions into the split-off band[3] [starting at $J_p(77\text{ K})+\Delta_{so}=0.396$ eV]. These two allowed absorption band components have not been taken into account by Ohta *et al.*[1] due to the confinement of their experimental data to energies $h\nu>0.43$ eV. We believe this is the reason for the different results obtained in this paper and in Ref. 1.

It may also be worthwhile to point out that in the present case of Si:V no significant contribution of allowed hole transitions into the heavy-hole band was detected. This is in contrast to our results obtained with Si:S (Ref. 41) and Si:Se.[42] In these cases, the corresponding electronic absorption cross sections $\tilde{\sigma}_p(h\nu)$ showed a rather simple (nearly linear) behavior over a relatively large energy interval at higher energies due to the strong contribution of hole transitions into the heavy-hole band.

This short discussion of some features in our detailed numerical analysis of optical data already shows that there are good reasons to believe that the present numerical results are more adequate than the ones suggested in Ref. 1. Unfortunately, this also means that the significant discrepancy between the lattice adjustment energy values detected from different sets of optical and electrical data is still not removed.

Attempting to remove a similar discrepancy in the case of the GaP:O center (state 1), Henry and Lang[39] assumed a relatively strong shift (about 22%) of the relevant phonon frequencies in both alternative charge states. We have tested this hypothesis in the present case of the *C* level in Si:V. To this end, we performed alternative fittings of the electrical data taken from Table I and Fig. 10 of Ref. 10, respectively, on the basis of the analytical framework for NMP transitions.[40,44,45] Using the same lattice adjustment energy, A_p, for the charge state ''empty'' (after hole capture) as the one obtained from our numerical analyses of optical data

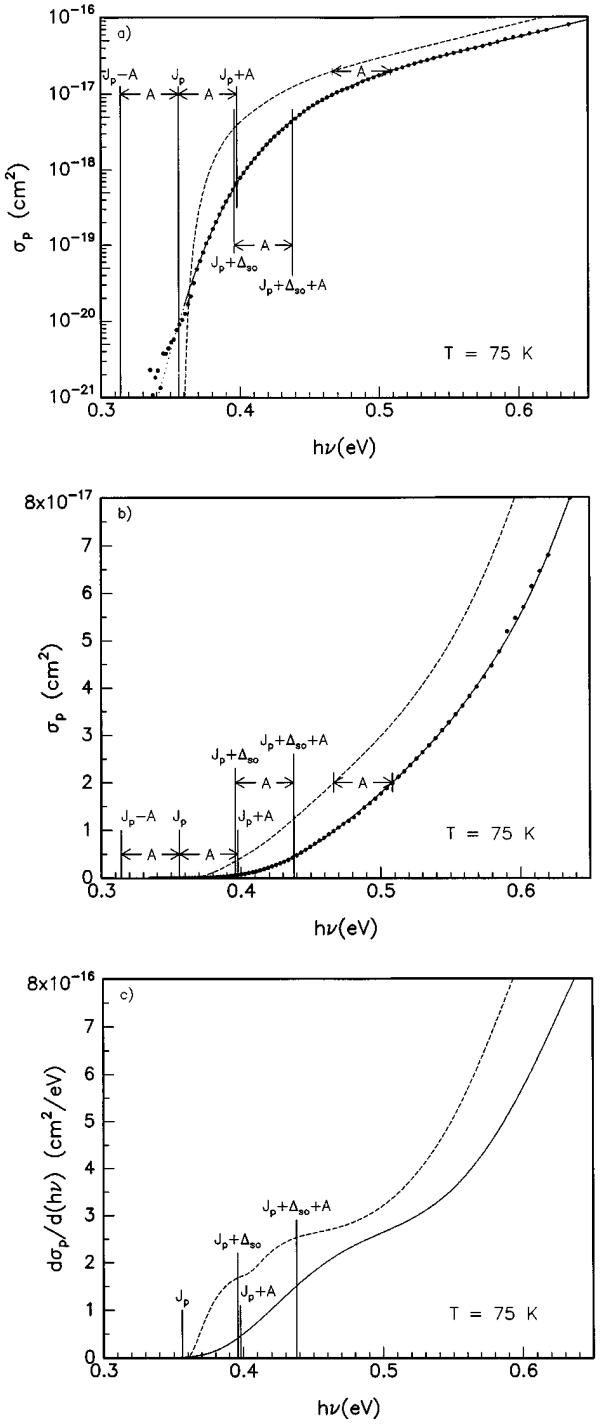

FIG. 10. Graphical representation of the numerical deconvolution of the total set of hole excitation cross-section data (Fig. 4 in combination with additional experimental points for $T=75$ K) on the basis of Eq. (21). (a) Measured $\sigma_p(h\nu, 75\text{ K})$ data (full curve) in comparison with the deconvoluted electronic part $\tilde{\sigma}_p(h\nu)$ (dashed curve) in logarithmic representation. (b) The same curves as in (a) but in linear representation. The magnitude of the Franck-Condon shift, $A=0.042$ eV, is directly obtained from the horizontal shift between the nearly linear region of the electronic cross section (dashed curve) and the convoluted $\sigma_p(h\nu, 75\text{ K})$ data (full curve). (c) First derivative of the convoluted absorption cross-section curve, $d\sigma(h\nu,75\text{ K})/d(h\nu)$ (full curve), and of the corresponding electronic part, $d\tilde{\sigma}(h\nu)/d(h\nu)$ (dashed curve). The latter has a steplike structure in the vicinity of the absorption threshold energy $J_p(77\text{ K})+\Delta_{so}=0.396$ eV for hole excitation into the split-off band.

[Fig. 9(a)], i.e., $A_p = 0.042$ eV [in Fig. 9(c)], an almost indistinguishable alternative fit of the total set of electrical data was obtained when using a lattice adjustment energy A_n of only 0.019 eV in charge state ''full'' (after hole emission). As shown in Fig. 9(c), this particular set of parameters is actually able to reducing the classical vibrational barrier for NMP hole capture to a similar value (of about 0.09–0.10 eV) as for the conventional model[10] with a large A value without any phonon frequency shift [Fig. 9(b)]. On the other hand, owing to the basic relationship $(\omega_n/\omega_p)^2 = A_n/A_p$ (Ref. 44) which connects phonon frequencies with lattice adjustment energies in both alternative charge states, the relatively strong reduction of A_n in comparison with A_p would require a corresponding phonon frequency reduction of about 33%, i.e., an even larger phonon frequency shift than the one postulated by Henry and Lang[39] in the case of GaP:O.

It is questionable as to whether or not such a large phonon frequency shift is physically realistic, especially for a trap in silicon for which lattice relaxation phenomena are considered to be significantly weaker than in other semiconductor materials.[9] Moreover, from presently available photoionization cross-section data (Fig. 4), there is no indication for such a large phonon frequency shift. Actually, we have analyzed these optical data (in analogy to Ref. 44) also in considerable detail on the basis of a generalized analytical framework[40] that, in principle, would allow the detection of phonon frequency shifts larger than about 10%. However, we have not found any indication of such a shift. Interestingly, this is again in analogy to the case of GaP:O where a similar numerical analysis[8,40] of experimental hole ionization cross-section data[23,24] has shown that the relevant lattice adjustment energies A_n and A_p are nearly the same in both charge states (in accordance with Refs. 23 and 24). In summary, from our detailed numerical analyses of the optical data for the presently studied case of the C level in Si:V (Fig. 4), it is concluded that the lattice adjustment energies A_n and A_p for both charge states range between 0.04 and 0.05 eV. Consequently, within the framework of the commonly considered picture (Fig. 9) of a single effective configuration coordinate, a phonon frequency shift considerably larger than 10% [cf. Fig. 9(c)] appears not to be plausible.

The existing discrepancy may, in principle, be removed by generalizing the existing theory of NMP transitions for cases for which frequency shifts of different modes may have different signs. Such a mechanism is, in principle, capable of reducing vibrational barriers significantly without requiring larger lattice adjustment energies. A possible further reduction of vibrational barriers at a fixed lattice adjustment energy can probably also be achieved by changing[46] the principal axes of oscillations in a corresponding multidimensional lattice oscillator coordinate space. Unfortunately, such generalizations seem to be rather difficult to be realized computationally. At present, no analytical framework is available which would enable such a quantitative analysis.

V. SUMMARY

In spite of numerous studies of deep levels in silicon, there is still only little quantitative information available on the actual temperature dependence of relevant level position parameters (i.e., zero-phonon binding energies and Gibb's free energies) and associated Franck-Condon shifts (lattice adjustment energies). The primary goal of the present paper was therefore to present an example of how such information is obtained from quantitative investigations. The present study of the C level in Si:V involved several new combinations of experimental measurements and theoretical analysis procedures. In view of their possible applications in forthcoming deep level studies, it may be useful to briefly summarize the characteristic methodological changes and differences in the present study.

(i) Electrical measurements of thermal emission rates and capture coefficients were performed at the same temperatures. This made a direct numerical calculation of Gibb's free energies possible without any intermediate exponential regressions or other approximate linearization procedures.

(ii) Carrier capture properties were quantified exclusively in terms of capture coefficients (of dimension $cm^3\ s^{-1}$) since these coefficients are primary data quantifying the capture properties of a deep trap. Moreover, they are directly related to the experimentally measured capture rates. In this way, one avoids the implication of carrier capture cross sections which are not directly measured.

(iii) Optical measurements, comprising, in particular, the theoretically significant low-energy tail regions, were performed at several temperatures.

(iv) Zero-phonon binding energies as well as an estimation of the associated Franck-Condon shift were determined by analyzing the temperature-dependent slopes and curvatures (thermal activation properties) of photoionization cross-section spectra tails.

(v) Evidence was given for the nonlinear (nearly quadratic) temperature dependence of the zero-phonon binding energy. This dependence can be described approximately by a Varshni-type analytical expression.

(vi) A simultaneous fitting and extension of the temperature dependence of Gibb's free energies and zero-phonon binding energies was performed on the basis of a unique set of parameters.

ACKNOWLEDGMENTS

The authors would like to thank the Swedish Board for Technical Development, the Swedish National Science Research Council, the Ministry of Science and Art of the Free State Saxony, and the German Research Community (DFG) for financial support, which made the collaboration between the Department of Solid State Physics of the University of Lund and the Institute of Physics of the Technical University Chemnitz-Zwickau possible. They would also like to thank Dr. F. Blaschta (TU Chemnitz-Zwickau) for preparing the figures.

*Electronic address: paessler@physik.tu-chemnitz.de

[1] E. Ohta, T. Kunio, Jr., T. Sato, and M. Sakata, J. Appl. Phys. **56**, 2890 (1984).

[2] L. Tilly, H. G. Grimmeiss, H. Pettersson, K. Schmalz, K. Tittelbach, and M. Kerkow, Phys. Rev. B **44**, 12 809 (1991).

[3] R. Pässler, Phys. Status Solidi B **179**, 133 (1993).

[4] Y. P. Varshni, Physica (Utrecht) **34**, 149 (1967).

[5] C. D. Thurmond, J. Electrochem. Soc. **122**, 1133 (1975).

[6] L. Tilly, H. G. Grimmeiss, H. Pettersson, K. Schmalz, K. Tittelbach, and M. Kerkow, Phys. Rev. B **43**, 9171 (1991).

[7] R. Pässler, Czech. J. Phys. B **24**, 322 (1974); **25**, 219 (1975).
[8] R. Pässler, Phys. Status Solidi B **186**, K63 (1994).
[9] G. F. Neumark and K. Kosai, in *Deep Levels, bias, Alloys, Photochemistry,* edited by R. Willardson and A. Beer, Semiconductors and Semimetals Vol. 19 (Academic, New York, 1983), p. 1.
[10] E. Ohta and M. Sakata, Solid State Electron. **23**, 759 (1980).
[11] D. V. Lang, J. Appl. Phys. **45**, 3014 (1974).
[12] H. G. Grimmeiss and C. Ovrén, J. Phys. E **14**, 1032 (1981).
[13] H. Pettersson (unpublished).
[14] W. Shockley and W. T. Read, Jr., Phys. Rev. **87**, 835 (1952).
[15] J. S. Blakemore, *Semiconductor Statistics* (Pergamon, New York, 1962).
[16] O. Engström and A. Alm, Solid State Electron. **21**, 1571 (1978).
[17] D. V. Lang, H. G. Grimmeiss, E. Meier, and M. Jaros, Phys. Rev. B **22**, 3917 (1980).
[18] R. Pässler, Phys. Status Solidi B **170**, 219 (1992).
[19] R. Pässler, Phys. Status Solidi B **158**, K143 (1990).
[20] R. Pässler, Phys. Status Solidi B **162**, K47 (1990).
[21] R. Pässler, Phys. Status Solidi B **167**, 165 (1991).
[22] A. A. Kopylov and A. N. Pikhtin, Fiz. Tverd. Tela (Leningrad) **16**, 1837 (1974) [Sov. Phys. Solid State **16**, 1200 (1975)].
[23] B. Monemar and L. Samuelson, Phys. Rev. B **18**, 809 (1978).
[24] L. Samuelson and B. Monemar, Phys. Rev. B **18**, 830 (1978).
[25] D. Bois and A. Chantre, Rev. Phys. Appl. **15**, 631 (1980).
[26] A. Chantre, G. Vincent, and D. Bois, Phys. Rev. B **23**, 5335 (1981).
[27] A. Nouailhat, F. Litty, S. Loualiche, P. Leyral, and G. Guillot, J. Phys. **43**, 815 (1982).
[28] S. Loualiche, A. Nouailhat, G. Guillot, and M. Lannoo, Phys. Rev. B **30**, 5822 (1982).
[29] B. K. Ridley, J. Phys. C **13**, 2015 (1980).
[30] R. Pässler, Phys. Status Solidi B **65**, 561 (1974).
[31] R. Pässler, Phys. Status Solidi B **68**, 69 (1975); **76**, 647 (1976).
[32] R. Pässler, Phys. Status Solidi B **86**, K39 (1978).
[33] B. K. Ridley, J. Phys. C **11**, 2323 (1978).
[34] B. K. Ridley, Solid State Electron. **21**, 1319 (1978).
[35] R. Pässler, Phys. Status Solidi B **85**, 203 (1978); **103**, 673 (1981).
[36] R. Pässler, Czech. J. Phys. B **34**, 377 (1984).
[37] J. Frenkel, Phys. Rev. **54**, 647 (1938).
[38] R. Pässler, Phys. Status Solidi B **83**, K55 (1977); **83**, K11 (1977).
[39] C. H. Henry and D. V. Lang, Phys. Rev. B **15**, 989 (1977).
[40] R. Pässler (unpublished).
[41] H. Pettersson, R. Pässler, F. Blaschta, and H. G. Grimmeiss, J. Appl. Phys. **80**, 5312 (1996).
[42] R. Pässler, H. Pettersson, and H. G. Grimmeiss, Semicond. Sci. Technol. **11**, 1388 (1996).
[43] R. Pässler, Phys. Status Solidi B **78**, 625 (1976).
[44] G. Meinhold, Thesis TU Chemnitz-Zwickau, 1984.
[45] A. Haug, *Theoretische Festkörperphysik II* (Deuticke, Wien, 1970).
[46] R. Kubo and Y. Toyozawa, Prog. Theor. Phys. **13**, 160 (1955).